Mayank Kalra
Mechanical and Mechatronics Engineering,
University of Waterloo,
Waterloo, ON N2L 3G1, Canada
e-mail: mayank.kalra@uwaterloo.ca

Robert Bahensky
Mechanical and Mechatronics Engineering,
University of Waterloo,
Waterloo, ON N2L 3G1, Canada
e-mail: ;robert.bahensky@uwaterloo.ca

Stewart D. McLachlin
Mechanical and Mechatronics Engineering,
University of Waterloo,
Waterloo, ON N2L 3G1, Canada
e-mail: ;stewart.mclachlin@uwaterloo.ca

Duane S. Cronin
Mechanical and Mechatronics Engineering,
University of Waterloo,
Waterloo, ON N2L 3G1, Canada
e-mail: ;dscronin@uwaterloo.ca

Naveen Chandrashekar[1]
Mechanical and Mechatronics Engineering,
University of Waterloo,
200 University Avenue West,
Waterloo, ON N2L 3G1, Canada
e-mail: nchandra@uwaterloo.ca

In-Situ Fracture Tolerance of the Metatarsals During Quasi-Static Compressive Loading of the Human Foot

Accidental foot injuries including metatarsal fractures commonly result from compressive loading. The ability of personal protective equipment to prevent these traumatic injuries depends on the understanding of metatarsal fracture tolerance. However, the in situ fracture tolerance of the metatarsals under direct compressive loading to the foot's dorsal surface remains unexplored, even though the metatarsals are the most commonly fractured bones in the foot. The goal of this study was to quantify the in situ fracture tolerance of the metatarsals under simulated quasi-static compressive loading. Fresh-frozen cadaveric feet ($n = 10$) were mounted into a testing apparatus to replicate a natural stance and loaded at the midmetatarsals with a cylindrical bar to simulate a crushing-type injury. A 900 N compressive force was initially applied, followed by 225 N successive load increments. Specimens were examined using X-ray imaging between load increments to assess for the presence of metatarsal fractures. Descriptive statistics were conducted for metatarsal fracture force and deformation. Pearson correlation tests were used to quantify the correlation between fracture force with age and body mass index (BMI). The force and deformation at fracture were 1861 ± 642 N (mean ± standard deviation) and 22.6 ± 3.4 mm, respectively. Fracture force was correlated with donor BMI ($r = 0.90$). Every fractured specimen experienced a transverse fracture in the second metatarsal. New biomechanical data from this study further quantify the metatarsal fracture risk under compressive loading and will help to improve the development and testing of improved personal protective equipment for the foot to avoid catastrophic injury.
[DOI: 10.1115/1.4052685]

Introduction

Foot and ankle injuries lead to a substantial amount of lost time at work, as well as many short- and long-term quality of life changes [1–3]. The National Safety Council reported that foot injuries in the United States accounted for 47,160 private-sector work-related injuries requiring time off from work in 2019 [4]. Fractures were the most common injury type and the metatarsals were the most frequently fractured bone, accounting for 28% of all fractures [4,5].

Approximately 10% of metatarsal injuries are caused by direct trauma to the metatarsals [6]. Hong et al. reported that the most common foot and ankle injury mechanism from forklift crush injuries in an industrial setting was a crush injury sustained from the wheels, which accounted for approximately 63% of all injuries [7]. A crushing-type injury to the foot occurs under a relatively low deformation rate when compared to an impact injury [7]. Numerous studies have investigated the incidence, classification, and treatment of metatarsal fractures [5,6,8,9]; however, studies related to characterizing the in situ fracture tolerance of the metatarsal bones are limited.

Strain and force measurements on the metatarsals have been performed during various activities using both experimental and computational approaches. Milgrom et al. implanted strain gages on the metatarsals of live participants and studied strains during gait [10]. Smolen and Quenneville examined the strains in different bones in the foot when a static compressive load was applied to the tibia, using a detailed and validated finite element model [11]. Fujikawa et al. previously studied the fracture tolerance of ursine metatarsals under quasi-static compressive loads and extrapolated the results to human feet using a numerical modeling approach [12]. Several studies have also investigated the mechanical properties and injury behavior of individual metatarsals ex situ (extracted from cadaveric human feet) under a variety of loading conditions [13–17]. However, these isolated strain measurements, numerical models, and cadaveric studies have not provided a full understanding of metatarsal injury behavior under more complex in situ loading, where the force is applied directly to the metatarsals. For example, it is currently unknown how much force is required to fracture the metatarsals or which metatarsal is most prone to fracture when subjected to in situ quasi-static compressive loading of an intact foot.

Investigation of the in situ fracture tolerance of the metatarsals under compressive loading applied directly to dorsal surface of the foot considers a practical workplace injury scenario and does not neglect the role of the surrounding structures within the foot. To our knowledge, there is currently no published literature on the fracture strength of human metatarsals when the forefoot is loaded under a compressive deformation. Moreover, metatarsal personal protective equipment standards established by the American Society for Testing and Materials incorporate drop impact loads and measure peak deformation without considering quasi-static loads and fracture strength of the foot [18]. By characterizing the metatarsal fracture tolerance, personal protective equipment such as metatarsal protectors can be developed to prevent injuries more effectively, along with providing new data to create or improve test standards for such protective equipment. To address the gap in metatarsal injury characterization, the goals of the current study were to: (1) measure and examine the low-rate compressive loading required to induce in situ metatarsal fractures using a cadaveric model and (2) develop a metatarsal injury risk curve based on the recorded fracture force measurements.

Methods

Specimen Details. The research study was approved by the Office of Research Ethics at University of Waterloo. Ten unpaired

[1]Corresponding author.
Manuscript received May 9, 2021; final manuscript received September 22, 2021; published online November 5, 2021. Assoc. Editor: Tishya Wren.

Table 1 Donor information with means and standard deviations ($n = 10$)

Specimen (ID #)	Age (years)	Sex	Height (cm)	Mass (kg)	BMI (kg·m^{-2})	Cause of death
1	59	F	155	36	15.1	Small bowel cancer
2	53	F	175	59	19.2	Renal disease/hypertension
3	58	M	175	72	23.6	Ischemic cardiomyopathy/diabetes Mellitus
4	58	M	198	83	21.4	Cardiopulmonary arrest and end stage liver disease
5	58	M	175	68	22.2	Cirrhosis of the liver with ascites
6	39	M	178	72	23.0	Frontal glioblastoma
7	58	M	201	106	26.5	Cardiorespiratory arrest/brain cancer with metastasis
8	42	M	191	86	23.7	Malignant neoplasm in part of the bronchus or lung
9	36	M	183	90	27.1	Unknown
10	50	M	188	167	47.5	Unknown
Mean	51.1		181.9	83.9	24.9	
SD	8.9		13.4	34.8	8.6	

BMI: body mass index calculated postdeath, SD: standard deviation.

fresh frozen cadaver feet (eight males, two females), sectioned approximately 100 mm above the ankle joint, were procured for this study. All donors were less than 60 years old and had no signs or histories of foot injury. Donor information for all specimens is shown in Table 1. The specimens were kept frozen until the day prior to the experiment.

Experimental Setup. A custom loading apparatus consisting of two linear electromechanical actuators was designed to load the cadaver feet (Fig. 1). The first actuator was a position-controlled lead-screw actuator (RSA32, Tolomatic Inc., Hamel, MN) oriented vertically and used to apply a compressive load to the forefoot of the specimens (labeled "A" in Fig. 1). The load was applied through a 25.4-mm diameter cylindrical steel indenter, following the American Society for Testing and Materials (ASTM International) standard for foot protection [18]. The indenter length was 127.0 mm with its longitudinal axis oriented parallel to the frontal plane (labeled "E" in Fig. 1). To ensure interspecimen consistency the frontal plane was approximated using anatomical landmarks including the proximal first to third phalanges and the malleoli. The applied compressive load was measured using a load cell (LC203-2K, ~8896 N capacity, Honeywell, Inc., Charlotte, NC) mounted in series between the actuator and indenter (labeled "C" in Fig. 1). The second actuator was a belt actuator (14 H, Macron Dynamics Inc., Croydon, PA) oriented in the anterior-posterior direction and used to adjust the location of the applied load (labeled "B" in Fig. 1).

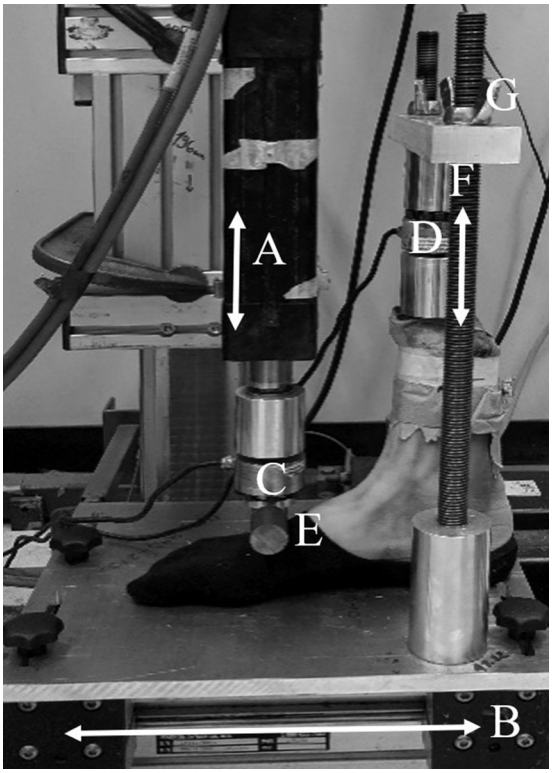

Fig. 1 Experimental metatarsal loading setup: (*a*) position-controlled vertical actuator to load the metatarsals, (*b*) position-controlled horizontal actuator to position the foot in anterior-posterior direction, (*c*) load cell to measure compressive load applied to metatarsals, (*d*) load cell to measure applied bodyweight load, (*e*) 25.4 mm diameter indenter positioned at first midmetatarsal, (*f*) vertical threaded rods to support the specimen and guide the horizontal member, and (*g*) wingnuts to apply compressive bodyweight load to the tibia

To simulate an in vivo weightbearing scenario, a mechanism was designed to apply a simulated bodyweight force to each specimen. A threaded rod was inserted into the intramedullary canal of the tibia, secured using a hardening resin, and fastened to a horizontal member. This member was supported on the baseplate by two vertical threaded rods (labeled "F" in Fig. 1) and a pair of wingnuts (labeled "G" in Fig. 1) were tightened to apply a compressive force to the specimen equal to half of the donor's reported bodyweight. An axial load cell (LC203-2K, ~8896 N capacity, Honeywell Inc, Charlotte, NC) connected in series between the tibial rod and horizontal member measured the applied bodyweight (labeled "D" in Fig. 1). LABVIEW software (National Instruments, Austin, TX) was used for the acquisition of all force data. With the exception of the insertion of the intramedullary rod the specimens were unaltered from their natural state.

Testing Protocol. Cadaveric specimens were thawed overnight and then prepared for attachment to the experimental setup. Prior to loading X-ray scans were taken for each specimen in the medial, lateral, plantar, and dorsal views (Phoenix v|tome|x s, General Electric Sensing and Inspection Technologies, Boston, MA). A three-dimensional (3D) microcomputed tomography (CT) scan (voxel size: 0.14 mm) was taken for each specimen to locate the mid-diaphysis of the first metatarsal and ascertain there were no prior metatarsal fractures. Each specimen was then mounted on the loading apparatus and positioned such that the indenter aligned with the mid-diaphysis of the first metatarsal, by using the distance from mid-diaphysis of the first metatarsal to the first distal phalanx, which was measured from the CT scan. To ensure intraspecimen consistency, the toes and heel of each foot were traced directly on the support platform prior to the first trial and served as reference guide for future trials.

In the first trial, a compressive load of approximately 900 N was applied to each specimen at a rate of 1 mm/s using the vertical actuator. This force was chosen as the initial value for all specimens based on tests to failure in two unrelated pilot specimens.

Table 2 Second metatarsal fracture forces, peak deformation, metatarsal cross-sectional area, and moment of inertia

Specimen (ID #)	Fracture force (N)	Peak vertical deformation (mm)	Mid-MT2 area (mm^2)	Mid-MT2 MOI (mm^4)	Fracture site area (mm^2)	Fracture site MOI (mm^4)
1	979	nr	43	240	29	134
2	988	18.3	51	415	32	233
3	1598	23.5	71	697	57	668
4	1624	28.9	60	271	64	352
5	1766	nr	50	410	31	230
6	2068	20.5	62	558	39	372
7	2478	23.7	74	417	56	284
8	2500	20.8	90	588	75	391
9	2749	22.2	54	318	50	347
10	DNF (>4653)	31.1	72	419	DNF	DNF

DNF: did not fracture, nr: not recorded, MOI: moment of inertia, MT2: second metatarsal.

The actuator displacement was held at the desired load for 12 s and then unloaded. Following the loading phase, the specimen was unloaded and removed from the testing apparatus and an X-ray scanning phase was conducted to check for metatarsal fractures. Fractures were identified by a visible crack in the bone when compared to the pretest X-ray scans. Fracture assessment was conducted by at least three researchers. In the absence of a fracture, a subsequent trial (consisting of an additional loading and scanning phase) was conducted with the peak load increased by approximately 225 N. Trials continued with 225 N load increments until a fracture was detected on the X-ray scan. If the presence of a fracture was uncertain, X-rays were sent to a collaborative orthopedic surgeon for confirmation. The fracture force was subsequently defined as the highest force sustained prior to detection of a fracture on the X-ray image or in combination with a large sudden decrease in the force-time history curve. The displacement of the indenter head was measured with a digital caliper (0.01 mm resolution) during the 12 s hold period to find the deformation of the foot at maximum loading relative to the unloaded state.

Data Analysis. The force-time history and peak deformation were recorded during each trial. Descriptive statistics were calculated for the fracture forces and deformations at fracture. A Shapiro–Wilks test was conducted on BMI and fracture force data. Using the 3D CT scans of the feet, geometric properties including cross-sectional area and second moment of area (moment of inertia) for the fractured metatarsals were calculated at the mid-diaphysis and at the fracture location using 3D Slicer (v4.10.2) and SOLIDWORKS 2021 (Dassault Systèmes SOLIDWORKS Corp., Waltham, MA). A Pearson correlation coefficient was used to identify whether the donor age, BMI, deformation at fracture, or geometric properties were correlated with the fracture force, as well as whether BMI was correlated with geometric properties. A survival analysis was conducted by censoring the data based on the presence or absence of a fracture, whereby all nonfracture peak force values were left-censored and fracture forces were either right-censored or classified as complete data. In the case of right-censored fractures, the error was at most 225 N due to the difference between successive load increases. The parameters for the survival curve were estimated using a lower cumulative Weibull probability distribution with 95% confidence intervals (CI). Fracture forces were determined at the 5, 10, 25, 50, and 95% probability levels, similar to the analysis performed by Yoganandan et al. [19].

Results

Nine specimens (ID# 1–9) sustained a fracture in the second metatarsal and one specimen (ID #1) sustained an additional fracture in the third metatarsal. In eight of the nine specimens, the fracture was detected solely on the X-ray image. In one specimen, the combined use of the X-ray image plus a large visible reduction (sudden dip) in the force-time curve indicated the onset of fracture. One specimen (ID# 10) did not exhibit any signs of fracture, even after a maximum possible load of 4653 N was applied.

The fracture force ($n = 9$), peak deformation ($n = 8$), as well as the geometric properties of the second metatarsals measured at the mid-diaphysis ($n = 10$) and at the fracture location ($n = 9$) are shown in Table 2. The geometric properties of the sole fractured third metatarsal from specimen ID# 1 was not examined since there were no other fractures at this location in the other specimens for comparison. The deformations at fracture for two specimens (ID# 1, 5) were missed and not recorded. A Shapiro–Wilks test showed BMI ($W(9) = 0.95$, $p = 0.633$) and fracture force ($W(9) = 0.93$, $p = 0.466$) were normally distributed.

The fractured specimens had a metatarsal fracture force of 1861 ± 642 N (mean ± SD) with a 95% CI of 1440-2280 N ($n = 9$), and a deformation at fracture of 22.6 ± 3.4 mm (mean ± SD) with a 95% CI of 20.4–24.8 mm ($n = 7$). A complete set of force-time history curves from a single specimen (ID# 3) are shown in Fig. 2, demonstrating an approximate load increase of 225 N ± 10% between each trial. It is important to note that specimen data shown in Fig. 2 sustained a maximum force without fracture of 1598 N in trial 4 and subsequently fractured under an applied load of 1231 N during Trial 5 (shown as a dip in the force-time curve). In this case, the fracture force was defined as the maximum force observed in Trial 4 (1598 N) since this was the largest force sustained by the specimen prior to fracture detection (confirmed on the trial 5 X-ray).

A nondisplaced transverse fracture was the predominant mode of failure in eight specimens, while both displaced and nondisplaced fractures occurred in specimen ID# 1. A typical fracture is

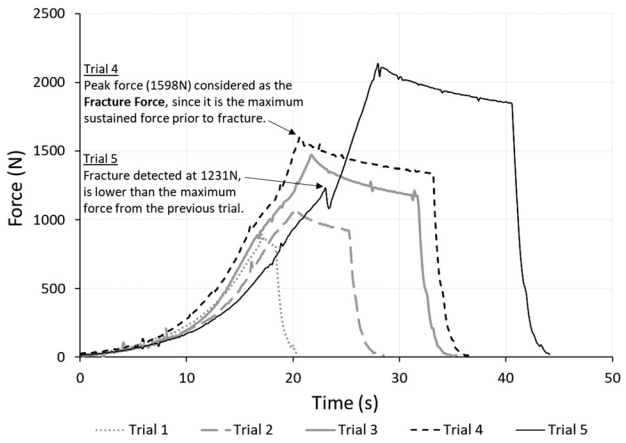

Fig. 2 Force time history curves of a typical specimen (specimen ID# 3 in Table 1). An initial load of 900 N was applied in trial 1, followed by a stepwise increase in each subsequent trial of approximately 225 N.

Fig. 3 A typical fracture (white arrow) of the metatarsal in the experiments. The dotted line shows the approximate line of application of the compressive load through the indenter.

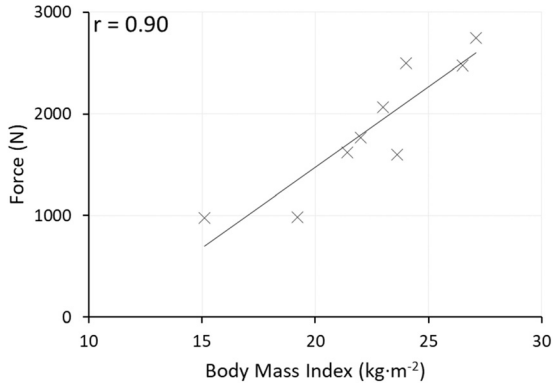

Fig. 4 Correlation between BMI and fracture force ($n = 9$, specimen ID# 10 excluded)

shown in Fig. 3. The correlation coefficients between the donor anthropometry and fracture force data suggest that the fracture force had very strong positive correlations with the donor BMI ($r = 0.90$, $p = 0.001$, $n = 9$), shown in Fig. 4. There were no significant correlations between fracture force with age ($r = 0.47$, $p = 0.073$, $n = 9$), midmetatarsal cross-sectional area ($r = 0.58$, $p = 0.101$, $n = 9$), midmetatarsal moment of inertia ($r = 0.22$, $p = 0.576$, $n = 9$), cross-sectional area at fracture location ($r = 0.58$, $p = 0.105$, $n = 9$), moment of inertia at fracture location ($r = 0.27$, $p = 0.485$, $n = 9$), or the deformation at fracture ($r = 0.06$, $p = 0.893$, $n = 7$). BMI was not significantly correlated with the deformation at fracture ($r = 0.133$, $p = 0.777$, $n = 7$) or any geometric properties including midmetatarsal cross-sectional area ($r = 0.44$, $p = 0.208$, $n = 10$), midmetatarsal moment of inertia ($r = 0.12$, $p = 0.746$, $n = 10$), cross-sectional area at fracture location ($r = 0.57$, $p = 0.113$, $n = 9$), or the moment of inertia at fracture location ($r = 0.49$, $p = 0.177$, $n = 9$).

Figure 5 shows the survival analysis curve and 95% CIs for the nine fractured specimens. The fracture forces associated with the 5, 10, 25, 50, and 95% fracture risk probabilities are 1115, 1458, 2083, 2842, and 4749 N, respectively.

Discussion

This study sought to address a knowledge gap in the characterization of in situ fracture tolerance of the forefoot under direct

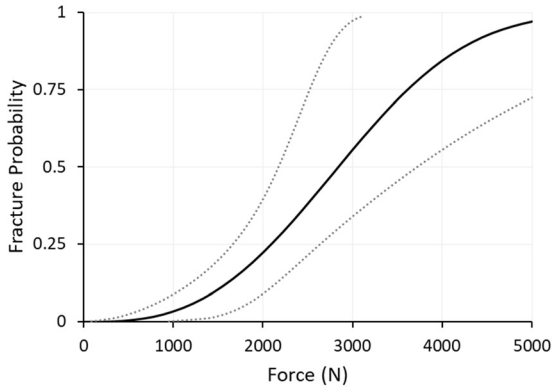

Fig. 5 Cumulative distribution function displaying injury risk along with a 95% confidence interval based on fracture force ($n = 9$, specimen ID# 10 excluded)

compressive loading. This mode of loading can occur during industrial accidents [3] and was replicated in the current study to better define the relationship between sustained loads and metatarsal fractures. The results of this work provide new important data regarding the fracture tolerance, fracture mechanism, deformation at fracture, and fracture risk probability of the metatarsals in situ.

In the tests conducted, the second metatarsal fractured in every specimen, except for specimen ID# 10 where no metatarsal fractures were observed. These findings are not consistent with the epidemiology of metatarsal fractures, which suggests that it is the smaller (third to fifth) metatarsals that fracture most often [6,20]. This inconsistency may exist because epidemiological studies take into consideration metatarsal fractures sustained during all types of loading scenarios, such as those encountered during automobile accidents or in athletes who fracture their fifth metatarsals due to overuse. In this study, the compressive load on the dorsal surface of the foot applies a direct load to metatarsals that are supported by soft tissues, which is a more complex boundary condition than simple three-point bending that has been applied in other studies. Danesi et al. reported that the second metatarsal has a lower bending stiffness than the first, third, or fourth metatarsals in the sagittal plane, and is the "longest and weakest" among all metatarsal bones [13]. These findings provide justification for the fracture mechanism observed in the current study. Since the compressive load was applied near the mid-diaphysis of the second metatarsal and the resulting fractures were transverse fractures, it is reasonable to suspect that the fractures were the result of excessive bending stress.

Direct comparison of the in situ results from this study to related work in this area is limited since no study to our knowledge has used a similar study design. Gutekunst et al. loaded isolated metatarsals from 10 elderly donors in three-point bending and reported a fracture force of 572 ± 299 N (mean $\pm$ standard deviation) for the second metatarsal [15], compared to the current study that identified a fracture force of 1861 ± 642 N. This increase in fracture tolerance is likely a result of the in situ loading, wherein the metatarsals were supported in the current study by surrounding structures that increased the overall load bearing capacity of the foot and distributed the load over the entire dorsal surface. Moreover, Gutekunst et al. [15] had specimens from seven female and three male donors with a mean age of 83 (range 56–99) years, whereas the current study had eight male and two female specimens with a mean age of 51 (range 39–59) years. While it is likely that testing isolated versus in situ metatarsals would alter the reported fracture force, in situ testing is more representative of the loading that would be seen in a compression type of foot injury. It is unknown how the younger mean specimen age in the current study affected the results compared to the older specimens tested in Ref. [15]. Prior work has investigated foot injuries using in situ and computational methodologies

[12,21–24]; however, Fujikawa et al. [12] is believed to be the only study to use an in situ quasi-static cadaveric methodology to predict the fracture tolerance of intact human metatarsals. Their prediction was made by extrapolating experimental results from ursine (bear) metatarsal specimens [12]. The study predicted "10% fracture risk probability" force values for six human females, with a mean of approximately 1700 N. While this value is similar to the mean fracture force observed in the current study, the methods used by Fujikawa et al. were dissimilar from the current methodology. Fujikawa et al. used the 10% ursine fracture probability and predicted human metatarsal fracture thresholds based on geometric differences in ursine versus human foot scans [12]. Moreover, the loading condition was different as their applied load was concentrated on a single metatarsal.

The specimens used in the current study were taken from donors less than 60 years in age (mean donor age: 51.1 years) to reflect the typical demographics of a working population for which this injury mechanism is relevant. While there was no statistically significant correlation ($p = 0.073$) between age and fracture force in the results from the current study, the results point toward a relationship between age and fracture force. Repeating this study with a larger donor age range, including both younger and older specimens, is necessary to determine the role of age more effectively in metatarsal fracture tolerance (for example, as it relates to the development of osteoporosis) along with the other reported factors for bone fracture tolerance.

There was a very strong correlation between donor BMI and fracture force ($r = 0.90$), as shown in (Fig. 4). Studies have shown that body frame dimensions are positively correlated with BMI [25] and that individuals with large frames tend to have higher bone mineral content and slightly greater amounts of absolute bone [26]. The large BMI of specimen ID# 10 is the probable reason the specimen did not experience any fractures. Furthermore, specimens with larger BMI also likely have higher amounts of fat and soft tissue, which could affect the resulting fracture force. However, the respective amounts of these soft tissues in each specimen were not quantified.

The loading rate used in the current study was 1 mm/s to represent a low-velocity quasi-static loading rate similar to other cadaveric studies [13,15]. While this rate may be slower than the loading rate experienced during an industrial accident, it was chosen to more precisely control the end of the loading phase when the target force for a trial was achieved. An alternative approach could have been to use a force-controlled loading phase, although this would have resulted in nonuniform strain rates and introduced potential viscoelastic effects. It is reasonable to suggest that the current methodology minimized viscoelastic behavior in the soft tissues of the foot. Figure 2 does show that during repeated loading cycles the ramp-up loading curves did not overlap potentially due to creep or permanent deformation of soft tissues; however, these small differences in the loading response would be unlikely to affect the resulting metatarsal fracture force.

The indenter used in the current study was chosen to replicate the test standards recommended by ASTM International to test metatarsal guards [18]. The use of a standardized indenter allows for other researchers to closely compare with the current experimental outcomes, while allowing metatarsal guard manufacturers to directly use these results to test and improve their products. For consistency, the load was centered on the first metatarsal as it is the initial metatarsal to be loaded during compression. It is crucial to note that most fractures occurred distal to the point of load application. Due to the in situ nature of testing, it is possible that the initial location of the metatarsal relative to the indenter may shift as the soft tissues are loaded and compressed. The orientation of the dorsal surface of the foot and geometry/asymmetry of the metatarsal may also play a role in fractures occurring away from the point of load application.

During metatarsal loading, each foot was subjected to an axial compressive load applied through the tibia equal to half the donor's bodyweight. This bodyweight load simulated a two-legged stance, ascertained a natural orientation of the metatarsals (and the rest of the foot) while the metatarsals were loaded, and ensured the load distribution within the structure of the foot was accurately represented. Instead of applying an identical axial compressive load, it was decided to scale the respective load for each specimen to the bodyweight of the donor to better account for interspecimen variability. Muscle forces were not considered in this study and may contribute to fracture resistance of the foot under real-world conditions.

While the peak deformation of the foot at fracture was measured in the experiments, there was no consistent trend between this deformation and fracture force. Foot deformation could depend on BMI related factors such as the amount of superficial adipose or muscle tissue, geometry (arch) of the foot, and the properties of supporting structures such as ligaments; yet, examining BMI and deformation at fracture did not show a strong correlation. Therefore, an investigation of the factors relating deformation at fracture to metatarsal fracture strength requires additional research.

This study is believed to be the first to examine the quasi-static in situ fracture tolerance of human metatarsals in the absence of footwear. The data presented provide valuable new information to better define metatarsal injury tolerance. The injury risk curve can be used to assess the likelihood that a metatarsal fracture will occur under a certain loading scenario. The fracture force and deformation data presented can be used by industrial footwear manufacturers to design and develop effective metatarsal guards. Currently, there are no accepted test standards to test the metatarsal guards for quasi-static loading conditions. While test standards for impact loading of foot protection devices exist [18], they may be inadequate for quasi-static loading because high-rate loading could overestimate the protection offered by metatarsal guards due to viscoelastic effects of certain polymer materials. The data presented in this study can be used to develop new test standards specific to quasi-static loading conditions. The data can also be used to validate pre-existing finite element foot models [11,14,22], which could then be used to study other injury scenarios and corresponding injury prevention strategies. Furthermore, it would also be relevant to investigate in situ metatarsal fracture strength with respect to footwear; this study presents a methodology and results for these types of studies to build upon in the future.

There are recognized limitations of the current work. The test procedure required repeated loading and unloading of the specimen to test for fracture. This repetition could result in some damage accumulation and elongation of soft tissues, thus altering the orientation of the bones over a series of trials. However, this incremental loading was necessary to ensure that the fracture load could be estimated within 225 N of the true value. This increment was chosen to minimize the number of trials needed and was estimated based on the fracture limits previously reported in literature. In addition, there was an uneven distribution of donor sexes due to the limited availability and small number of cadaveric specimens acquired. Finally, the fracture forces reported here are representative of the specific loading scenario applied (which is a uniform compressive load using a 25.4 mm cylindrical bar loaded at 1 mm/s). If the loading orientation, indenter geometry, or loading rate were altered, these would have likely affected the fracture forces and resultant injury risk curve. Future investigations should assess fracture tolerance using other geometries, such as flat or oblique indenters and additional loading rates.

Conclusion

In summary, fracture tolerance tests were performed on 10 intact human cadaver feet to determine the force required to fracture the metatarsals. In-situ fractures consistently occurred at the second metatarsal with a mean fracture force of 1861 ± 642 N. An injury risk curve was developed using the experimental data, which predicted 2842 N as the compressive force associated with

a 50% fracture probability. The metatarsal fracture force was directly related to higher subject BMI values. Ultimately, the fracture tolerances and deformations at fracture obtained in this work provide new insights into metatarsal fracture risk. The data from this study could be used to foster safer workplaces and work practices by reducing the risk of metatarsal injury through the development and assessment of protective footwear devices and testing standards for traumatic metatarsal injury prevention.

Acknowledgment

We wish to thank Dr. Wanis Nafo for assistance with X-ray imaging.

Funding Data

- Natural Science and Engineering Research Council, Canada (Grant No. 533149-18; Funder ID: 10.13039/501100000038).
- Swenco Inc.

References

[1] Conti, S. F., and Silverman, L., 2002, "Epidemiology of Foot and Ankle Injuries in the Workplace," Foot Ankle Clin., **7**(2), pp. 273–290.

[2] Oleske, D. M., Hahn, J. J., and Leibold, M., 1992, "Work-Related Injuries to the Foot. Data From an Occupational Injury/Illness Surveillance System," J. Occup. Med., **34**(6), pp. 650–655.

[3] Vora, A., and Myerson, M. S., 2002, "Crush Injuries of the Foot in the Industrial Setting," Foot Ankle Clin., **7**(2), pp. 367–383.

[4] 2017, *Injury Facts*, Bureau of Labor Statistics, National Safety Council, Itasca, IL.

[5] Shibuya, N., Davis, M. L., and Jupiter, D. C., 2014, "Epidemiology of Foot and Ankle Fractures in the United States: An Analysis of the National Trauma Data Bank (2007 to 2011)," J. Foot Ankle Surg., **53**(5), pp. 606–608.

[6] Petrisor, B. A., Ekrol, I., and Court-Brown, C., 2006, "The Epidemiology of Metatarsal Fractures," Foot Ankle Int., **27**(3), pp. 172–174.

[7] Hong, C. C., Nashi, N., Kuan, W. S., Teh, J. W. D., and Tan, K. J., 2015, "Forklift-Related Crush Injuries of the Foot and Ankle," Foot Ankle Int., **36**(7), pp. 806–811.

[8] Buddecke, D. E., Polk, M. A., and Barp, E. A., 2010, "Metatarsal Fractures," Clin. Podiatr. Med. Surg., **27**(4), pp. 601–624.

[9] Miller, C. M., Winter, W. G., Bucknell, A. L., and Jonassen, A. E., 1998, "Injuries to the Midtarsal Joint and Lesser Tarsal Bones," J. Am. Acad. Orthop. Surg., **6**(4), pp. 249–258.

[10] Milgrom, C., Finestone, A., Sharkey, N., Hamel, A., Mandes, V., Burr, D., Arndt, A., and Ekenman, I., 2002, "Metatarsal Strains Are Sufficient to Cause Fatigue Fracture During Cyclic Overloading," Foot Ankle Int., **23**(3), pp. 230–235.

[11] Smolen, C., and Quenneville, C. E., 2017, "A Finite Element Model of the Foot/Ankle to Evaluate Injury Risk in Various Postures," Ann. Biomed. Eng., **45**(8), pp. 1993–2008.

[12] Fujikawa, T., Asano, Y., Nishimoto, T., and Nishikata, R., 2017, "Static Fracture Tolerance of Human Metatarsal in Being Run Over by Robot," IEEE/RSJ International Conference on Intelligent Robots and Systems (IROS), IEEE, Vancouver, BC, Canada, Sept. 24–28, pp. 6935–6942.

[13] Danesi, V., Cristofolini, L., Juszczyk, M. M., Erani, P., and Viceconti, M., 2012, "Mechanical Properties of the Human Metatarsal Bones," J. Mech. Med. Biol., **12**(4), p. 1250062.

[14] Fung, A., Loundagin, L. L., and Edwards, W. B., 2017, "Experimental Validation of Finite Element Predicted Bone Strain in the Human Metatarsal," J. Biomech., **60**, pp. 22–29.

[15] Gutekunst, D. J., Patel, T. K., Smith, K. E., Commean, P. K., Silva, M. J., and Sinacore, D. R., 2013, "Predicting Ex Vivo Failure Loads in Human Metatarsals Using Bone Strength Indices Derived From Volumetric Quantitative Computed Tomography," J. Biomech., **46**(4), pp. 745–750.

[16] Kwon, J. Y., Campbell, J. T., Myerson, M. S., and Jeng, C. L., 2011, "Effect of a Steel Toe Cap on Forefoot Injury Pattern in a Cadaveric Model," Foot Ankle Int., **32**(4), pp. 443–447.

[17] Masson, C., Thollon, L., Cesari, D., and Brunet, C., 2006, "Effects of Static High Compression on Human Foot-Ankle: Biomechanical Response and Injuries," Surg. Radiol. Anat., **28**(1), pp. 46–53.

[18] ASTM International, 2018, *Standard Test Methods for Foot Protection*, ASTM International, West Conshohocken, PA, Standard No. F2413-18.

[19] Yoganandan, N., Arun, M. W. J., Pintar, F. A., and Banerjee, A., 2015, "Lower Leg Injury Reference Values and Risk Curves From Survival Analysis for Male and Female Dummies: Meta-Analysis of Postmortem Human Subject Tests," Traffic Inj. Prev., **16**(sup1), pp. S100–S107.

[20] Cakir, H., Van Vliet-Koppert, S. T., Van Lieshout, E. M. M., De Vries, M. R., Van Der Elst, M., and Schepers, T., 2011, "Demographics and Outcome of Metatarsal Fractures," Arch. Orthop. Trauma Surg., **131**(2), pp. 241–245.

[21] Yoganandan, N., Pintar, F. A., Kumaresan, S., and Boynton, M., 1997, "Axial Impact Biomechanics of the Human Foot-Ankle Complex," Axial Impact Biomech. Human Foot-Ankle Complex, **119**(4), pp. 433–437.

[22] Gallenberger, K., Yoganandan, N., and Pintar, F., 2013, "Biomechanics of Foot/Ankle Trauma With Variable Energy Impacts," Ann. Adv. Automot. Med., **57**, pp. 123–132.

[23] Parenteau, C. S., Viano, D. C., and Petit, P. Y., 1998, "Biomechanical Properties of Human Cadaveric Ankle-Subtalar Joints in Quasi-Static Loading," ASME J. Biomech. Eng., **120**(1), pp. 105–111.

[24] Shin, J., and Untaroiu, C. D., 2013, "Biomechanical and Injury Response of Human Foot and Ankle Under Complex Loading," ASME J. Biomech. Eng., **135**(10), p. 101008.

[25] Henneberg, M., and Ulijaszek, S. J., 2010, "Body Frame Dimensions Are Related to Obesity and Fatness: Lean Trunk Size, Skinfolds, and Body Mass Index," Am. J. Hum. Biol., **22**(1), pp. 83–91.

[26] Chumlea, W. C., Wisemandle, W., Guo, S. S., and Siervogel, R. M., 2002, "Relations Between Frame Size and Body Composition and Bone Mineral Status," Am. J. Clin. Nutr., **75**(6), pp. 1012–1016.